SUPPORTING INFORMATION

Mix and Match: Co-assembly of Amphiphilic Dendrimers and Phospholipids Creates Robust, Modular and Controllable Interfaces

Samuel S. Hinman,[†] Charles J. Ruiz,[‡] Yu Cao,[§] Meghann C. Ma,[‡] Jingjie Tang,[§] Erik Laurini,[≠] Paola Posocco,[≠] Suzanne Giorgio,[§] Sabrina Pricl,[≠] Ling Peng,[*§] and Quan Cheng[*†,‡]

[†]Environmental Toxicology and [‡]Department of Chemistry, University of California – Riverside, Riverside, California 92521, USA
[§]Aix-Marseille University, CNRS, Centre Interdisciplinaire de Nanoscience de Marseille, CINaM UMR 7325, Equipe Labellisée Ligue Contre le Cancer, Marseille Cedex 09, France
[≠]Molecular Simulation Engineering (MOSE) Laboratory, Department of Engineering and Architecture (DEA), Trieste University, 34127 Trieste, Italy

*Email: quan.cheng@ucr.edu; ling.peng@univ-amu.fr

EXPERIMENTAL METHODS

Materials and Reagents. Triton X-100 was from Sigma-Aldrich (St. Louis, MO). Sulfo-NHS-Biotin, NHS-AMCA, and Streptavidin were from Pierce Biotechnology (Rockford, IL). Octadecyl Rhodamine B chloride (R18) was from Biotium Inc. (Hayward, CA). 1-palmitoyl-2-oleoyl-*sn*-glycero-3-phosphocholine (POPC) and 1-palmitoyl-2-6-[(7-nitro-2-1,3-benzoxadiazol-4-yl)amino]hexanoyl-*sn*-glycero-3-phosphocholine (NBD-PC) were from Avanti Polar Lipids (Alabaster, AL). BK-7 glass substrates were from Corning (Painted Post, NY). Chromium and gold used for electron-beam evaporation were acquired as pellets of 99.99% purity from Kurt J. Lesker (Jefferson Hills, PA).

Instrumentation. A dual-channel SPR spectrometer, NanoSPR5-321 (NanoSPR, Chicago, IL) with a GaAs semiconductor laser light source (λ_{max} = 670 nm) was used for all real-time binding measurements. SPR experiments were conducted at ambient temperature (~23 °C), with 1×PBS (10 mM Na_2HPO_4, 1.8 mM KH_2PO_4, 137 mM NaCl, 2.7 mM KCl, pH 7.4) used as the running buffer set to a flow rate of 5 mL/h unless otherwise noted. The transmission electron microscope (TEM) used was a JEOL 3010 microscope operating at 300 kV and a pole piece (Cs = 1.4 mm) giving a resolution of 0.21 nm. All TEM images were recorded at low irradiation doses ($<3\times10^3$ A•m^{-2}). Dynamic and electrophoretic light scattering were conducted with a Delsa Nano C particle analyzer (Beckman Coulter, Brea, CA). Fluorescence microscopy was carried out on an inverted Leica TCS SP5 II (Leica Microsystems, Buffalo Point, IL) using the 405 nm diode laser (for AMCA), 488 nm Argon laser line (for NBD), or 543 nm HeNe laser (for R18) in conjunction with a 40× (NA 1.1) objective and Leica HyD hybrid detector.

SPR Chip Fabrication. BK-7 glass microscope slides were first cleaned using a boiling piranha solution (3:1 v/v H_2SO_4 and 30% H_2O_2) for 30 min, followed by rinsing with DI water and drying under compressed air. 2 nm of chromium (0.5 Å/s), followed by 46 nm of gold (1.0 Å/s) were then deposited using electron-beam evaporation (Temescal, Berkeley, CA) at 5×10^{-6} Torr in a Class 1000 cleanroom facility (UCR Center for Nanoscale Science & Engineering). To obtain a hydrophilic surface for lipid bilayer formation, *ca.* 4 nm of SiO_2 was deposited on top of the gold layer using plasma enhanced chemical vapor deposition (PECVD) with a Unaxis Plasmatherm 790 system (Santa Clara, CA).

Synthesis and Characterization of Amphiphilic Dendrimers. The amphiphilic dendrimers **1**, **2** and **3** were synthesized according to the previously reported method (Scheme S1).[1] The chemical reagents used were purchased from Acros, Aldrich or Alfa Aesar. The ^{1}H NMR and ^{13}C NMR spectra were recorded at 300 MHz and 150 MHz respectively on Varian Mercury-VX300 and 600 spectrometers at room temperature. Coupling constants (*J*) are reported in Hertz, and chemical shifts are reported in parts per million (ppm) with TMS as an internal reference. FAB and ESI mass spectra were determined using ZAB-HF-3F or Finnigan LCQ Advantage mass respectively. MALDI-TOF mass spectra were recorded on a Voyager DE-STR. IR spectra were recorded with a Nicolet 380 spectrophotometer. Methyl acrylate, ethylenediamine, tetrahydrofuran were distilled before use. All other reagents and solvents were used without further purification from commercial sources. The dendron parts **G0.5, G1.5**, **G2.5,**[1] dendrimer parts **D1, D2**, **D3**[1] and alkyl azide compounds **C18**[2] were all synthesized according to the literature.

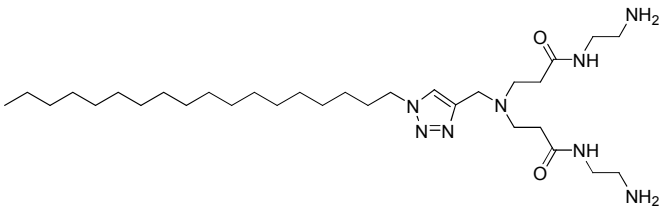

1

1: To a solution of **D1** (188 mg, 0.360 mmol) in methanol (5.00 mL) was added ethylenediamine (1.00 mL, 15.0 mmol). The reaction mixture was stirred under argon for 48 h at 30 °C until the IR analysis showed the complete consumption of **D1**. The reaction solution was evaporated, and the obtained residue was purified by precipitation with CH_3OH/Et_2O three times, yielding **1** (181 mg, 87%) as white solid. ^{1}H NMR (600 MHz, $CDCl_3$): δ 7.53 (br s, 2H, NH), 7.48 (s, 1H, CH), 4.32 (t, 2H, *J* = 7.2 Hz, CH_2), 3.76 (s, 2H, CH_2), 3.26-3.29 (m, 4H, CH_2), 2.76-2.82 (m, 8H, CH_2), 2.43 (t, 4H, *J* = 6 Hz, CH_2), 1.87-1.90 (m, 2H, CH_2), 1.25 (br, 30H, CH_2), 0.88 (t, 3H, *J* = 6.9 Hz, CH_3); ^{13}C NMR (150 MHz, $CDCl_3$): δ 172.9, 143.8, 122.8, 50.6, 50.0, 48.3, 42.0, 41.4, 34.4, 32.2, 30.6, 29.9, 29.8, 29.7, 29.6, 29.2, 26.7, 22.9, 14.4; IR (cm^{-1}): υ 1654.1; HRMS: calcd. for $C_{31}H_{63}N_8O_2^+$ $[M+H]^+$ 579.5069, found 579.5058.

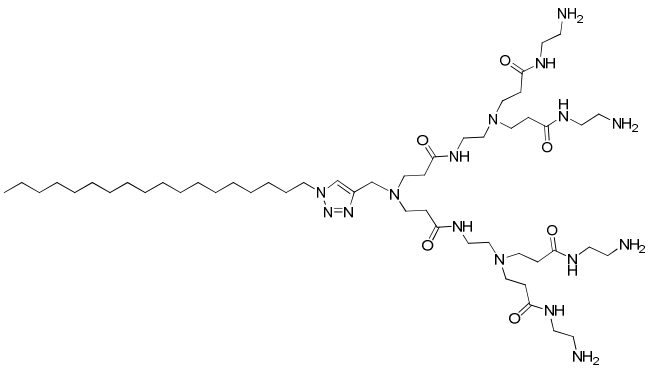

2

2: To a solution of **D2** (99.8 mg, 0.108 mmol) in methanol (5.00 mL) was added ethylenediamine (1.00 mL, 15.0 mmol). The reaction mixture was stirred under argon for 72 h at 30 °C until the IR analysis showed the complete consumption of **D2**. The reaction solution was evaporated, and the obtained residue was purified by precipitation with CH_3OH/Et_2O three times, yielding **2** (107 mg, 96%) as white solid. ^{1}H NMR (300 MHz, CD_3OD): δ 7.92 (s, 1H, CH), 4.39 (t, 2H, *J* = 7.1 Hz, CH_2), 3.81 (s, 2H, CH_2), 3.25-3.27 (m, 12H, CH_2), 2.73-2.80 (m, 20H, CH_2), 2.56 (t, 4H, *J* = 6.5 Hz, CH_2), 2.34-2.45 (m, 12H, CH_2), 1.89 (br, 2H, CH_2), 1.27 (br, 30H, CH_2), 0.89 (t, 3H, *J* = 6.6 Hz, CH_3); ^{13}C NMR (75 MHz, CD_3OD): δ 175.6, 175.0, 145.0, 125.5, 53.7, 51.6, 51.4, 50.7, 42.9, 42.2, 38.8, 35.1, 34.9, 33.4, 31.7, 31.1, 30.8, 30.4, 27.8, 24.1, 14.8; IR (cm^{-1}): υ 1643.82; HRMS: calcd. for $C_{51}H_{104}N_{16}O_6^{2+}$ $[M+2H]^{2+}$ 518.4157, found 518.4142.

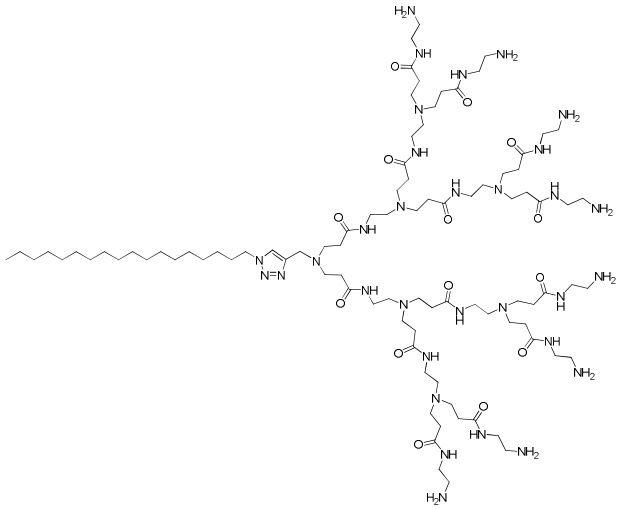

3

3: To a solution of **D3** in methanol was added ethylenediamine. The reaction mixture was stirred under argon for 72 h at 30 °C until the IR analysis showed the complete consumption of the ester

strating material. The reaction solution was evaporated, and the obtained residue was purified by precipitation with CH_3OH/Et_2O three times, yielding the corresponding amine products. **3** was obtained with a yield of 95%. ^{1}H NMR (600 MHz, CD_3OD): δ 7.90 (s, 1H, CH), 4.38 (t, 2H, J = 7.2 Hz, CH_2), 3.80 (s, 2H, CH_2), 3.22-3.24 (m, 28H, CH_2), 2.72-2.79 (m, 44H, CH_2), 2.55-2.57 (m, 12H, CH_2), 2.34-2.42 (m, 28H, CH_2), 1.88 (br, 2H, CH_2), 1.26 (br, 30H, CH_2), 0.88 (t, 3H, J = 7.2 Hz, CH_3); ^{13}C NMR (150 MHz, CD_3OD): δ 174.0, 173.6, 173.5,143.6, 124.0, 53.4, 52.3, 50.2, 49.9, 49.3, 41.7, 41.5, 40.8, 37.4, 33.6, 31.9, 30.2, 29.6, 29.4, 29.3, 28.9, 26.4, 22.5, 13.3; IR (cm^{-1}): υ 1644.60; HRMS: calcd. for $C_{91}H_{184}N_{32}O_{14}^{2+}$ $[M+2H]^{2+}$ 975.2343, found 975.2353.

Vesicle Preparation. An appropriate amount of POPC and/or dendrimer stock solution in chloroform was dried in a glass vial under nitrogen to form a thin lipid film. The vial containing lipids was then placed in a vacuum desiccator for at least 2 h to remove any residual solvent. The dried lipids were resuspended in 1×PBS to a lipid concentration of 1.0 mg/mL. After vigorous vortexing to remove all lipid remnants from the vial wall, the solution was bath sonicated for 30 min. Thereafter, the supernatant was extruded through a polycarbonate filter (Whatman, 100 nm) to produce small, unilamellar vesicles (SUVs) of uniform size. For fluorescence analysis, vesicle preparation followed the same procedure with the addition of 2% (w/w) NBD-PC, and dendrimer micelles were prepared with 1% (w/w) R18. All vesicle suspensions were used within one week and stored at 4 °C.

Fluorescence Microscopy. Fluidity of membranes incorporating the amphiphilic dendrimers was examined using fluorescence recovery after photobleaching (FRAP). Supported lipid bilayers were formed on clean glass coverslips (Fisher Scientific, Pittsburgh, PA) using vesicle suspensions deposited in 4.5 mm PDMS wells on the glass surface. These were incubated for 1 h prior rinsing with copious amounts of nanopure water. To assist with identification of the bilayer focal plane, a peripheral scratch in the bilayer was made. Photobleaching at 1.5 mW for 500 ms and fluorescence recovery monitoring were set up and performed using the LAS AF software package as described previously.[3-5]

FRAP Analysis. The methods of Axelrod and Soumpasis were applied to derive diffusion coefficients for each membrane.[3-4] First, the fluorescence intensity of each bleach spot was normalized over a background area of the same size to account for background photobleaching. This normalized value (F_n) was then used within the following formula to obtain the FRAP ratio (F_{FRAP}), with F_0 being the normalized intensity of the bleached area immediately after bleaching.

$$F_{FRAP} = \frac{F_n - F_0}{1 - F_0}$$

Thereafter, F_{FRAP} was plotted against time and fitted to a first order exponential function. The diffusion coefficient was calculated using the following equation, with *D* being the diffusion coefficient, ω the full width at half maximum of the focused Gaussian laser profile, $t_{1/2}$ the half-time recovery obtained from the exponential fit, and γ a correction factor accounting for the laser beam geometry.

$$D = \frac{\omega^2}{4t_{1/2}}\gamma$$

TEM Imaging. POPC and dendrimers were mixed from chloroform stocks, as in the other SUV procedures. 100 μL of a POPC solution (10 mg/mL) was combined with 50 μL of **1** (0.76 mg/mL), 50 μL of **2** (1.36 mg/mL), or 100 uL of **3** (1.28 mg/mL) and dried in a glass vial under nitrogen to form a thin lipid film. The vial containing the lipid/dendrimer mixture was then placed in a vacuum desiccator for at least 2 h to remove any residual solvent. Then, 1 mL D.I. water was added to the dried lipid/dendrimer film. After vigorous vortexing to remove all lipid remnants from the vial wall, the solution was bath sonicated for 30 min, then equilibrated 2 h at 277 K before being subjected to extrusion through a polycarbonate filter (Whatman, 200 nm). Thereafter, 100 μL of this solution was withdrawn and diluted 40× with D.I. water. After equilibration (15 min), 4 μL of the diluted solution were dropped onto a standard carbon-coated copper TEM grid and allowed to dry in an oven set to 310 K for 30 min. The grid was stained with 3 μL of uranyl acetate (2% in 50% EtOH) for 5 s, and the excess uranyl acetate was removed by filter paper. The dried specimens were observed with a JEOL 3010 transmission electron microscope operating at 300 kV. Data were analyzed with Digital Micrograph software.

Molecular Simulations

Dissipative Particle Dynamics (DPD) and Mesoscopic Bead-Field Hybrid (MBFH) Method. The simulations in this paper are based on DPD, a mesoscopic coarse-grained simulation method routinely employed for soft materials and biomembrane-containing system calculations.[6-7] The DPD particles (or beads), each representing a group of small molecules or extensive molecular fragments, interact by conservative, dissipative, and random forces, which are pairwise additive.[8]

The net force acting on a bead i can be expressed as $F_i = \sum_{j \neq i} (F_{ij}^C + F_{ij}^D + F_{ij}^R)$ and is calculated by summation over all other particles within a certain cutoff radius, r_c, which gives the extent of the interaction range. r_c, m, and k_BT are the unit distance, the particle mass, and the thermal energy, respectively.

The conservative force represents the excluded volume interactions between particles i and j in the dimensionless form $F_{ij}^C = a_{ij} (1 - r_{ij}) \hat{r}_{ij}$, where $r_{ij} = r_i - r_j$, $r_{ij} = |r_{ij}|$, $\hat{r}_{ij} = r_{ij}/r_{ij}$, a_{ij} is the maximum repulsion between particles i and j. The dissipative, $F_{ij}^D = -\gamma\, \omega(r_{ij})^2 (\hat{r}_{ij} \cdot v_{ij})\, \hat{r}_{ij}$, and random forces, $F_{ij}^R = \sigma\, \omega(r_{ij})\, \hat{r}_{ij}\, \zeta/(\delta t)^{-1/2}$, act as heat sink and source, respectively, and the combined effect of the two forces performs as a thermostat, where γ is a friction coefficient related to the thermal noise amplitude σ via the fluctuation−dissipation theorem, $\sigma^2 = 2\gamma k_B T$, $\omega(r)$ is a weight function, ζ is a normally distributed random variable with zero mean and unit variance that is uncorrelated for different particle pairs, δt is the time step of an integration scheme, and $v_{ij} = v_i - v_j$ is the relative velocity of the i^{th} and the j^{th} particles. The equations of particle motion, $dr_i/dt = v_i$ and $dv_i/dt = F_i$, are solved using as integration scheme the velocity-Verlet algorithm.

Finally, when modeling chains two additional forces are acting between bonded beads: a harmonic spring connecting two adjacent particles i and j $F_{ij}^b = k_b(r_{ij} - r_0)\, \hat{r}_{ij}$, where k_b is a spring constant and r_0 the equilibrium distance between the particles, and $F_{ijz}^\theta = 1/2\ k_\theta\ (1\text{-}\cos(\theta_0\text{-}\theta_0))$, where k_θ is a spring constant and θ_0 the equilibrium angle between adjacent beads triples ijz in a row.

In addition, large scale simulations of hybrid liposomes were performed employing the MBFH method[9] as implemented in *Culgi* (v.9.0, Culgi B.V., Leiden, The Netherlands). From a conceptual viewpoint, the hybrid method allows for different representations of constituents, either coordinate-based (bead) or continuous (bead concentration fields) in a single simulation volume, thus combining the computational efficiency of a field description (for the abundant solvent) with the explicit particle model (for the lipids and dendrons) and overcoming the restrictions of the individual methods. Thus, the MBF-hybrid free energy combines the free energy of a pure field-based system, $F^f[\{\rho_j\}]$, the potential energy of a pure particle-based system $V^B(\{r_i\})$, and a hybrid coupling interaction free energy $F^{Cp}[\{\rho_j\},\{r_i\}]$. The free energy is

$$F = F^f[\{\rho_j\}] + V^B(\{r_i\}) + F^{Cp}[\{\rho_j\},\{r_i\}]$$

The explicit expression for the coupling free energy is

$$F^{Cp} = \sum_{jk} c_{ji} \int_V \rho_j K(|r - r'_i|) dr$$

which introduces the hybrid coupling parameters c_{ji} for the binary interaction between a particle *i* and a field *j*; *K* is a normalized Gaussian kernel.

Accordingly, the total force acting on a bead *i* consists in the same forces in DPD plus the new coupling force F_i^{Cp}

$$F_i{}^{Cp} = -\sum_j c_{ji} \nabla K dr$$

and the contribution to the mean-field chemical potential is

$$\mu_{MF_i}{}^{Cp} = \sum_i c_{ji} K(r - r_i)$$

The coarse-grained models of dendron **1**-**3** reported in Figure S7 were adopted from our recent work.[10] A bead type C was used as the hydrophobic chain building block, a neutral bead type P and a positively charged bead type PC were employed for the non-protonated and terminal charged repeating unit of the dendron, respectively. A further bead type, L, links the hydrophilic and hydrophobic parts together.

In our simulations, each amphiphilic POPC molecule consists of a head group that contains three connected hydrophilic beads (H), and two tails with respective three hydrophobic beads per tail (T) following the model proposed by Ding et al.[11] for lipid membranes.

In explicit solvent calculations (DPD), water molecules were simulated by single bead type W, and an appropriate number of counterions of a charge of ± 1 were added to preserve charge neutrality and to account for the experimental solution ionic strength. In MBFH simulation, water was model a single Gaussian bead.

On the basis of the models described above, the phosphocoline/dendron **1**-**3** systems were simulated in a cubic box (maximum cell length L = 176) under periodic boundary conditions in three directions using the MBFH method. The hybrid dendrimer/POPC vesicles were pre-assembled imposing a random distribution between the two components (i.e., POPC and dendron). The calculations thereby describe the morphology assumed after thermodynamic equilibration of the components, and representative graphs showing the potential energy and

diameter as a function of simulation time for 3/POPC can be seen in Figure S8. Initially, the solvent field was equilibrated by means of dynamic density functional theory[12] with a diffusion factor of 0.05 and all the beads fixed. In the second step the bead diffusion was turn on (diffusion factor 0.02), and a full hybrid MBF simulation was performed until the system was equilibrated for $O(10^6)$ simulation steps with a time step of $\Delta t = 0.02\tau$.

In an attempt to imitate the SPR experiment at the mesoscale level we modeled the solid silica support as a rigid, non-interacting wall of $50r_c$ x $50r_c$.[13] A POPC bilayer (≈ 3500 molecules determined based on the head group area for POPC a = 0.68nm^2)[14] was initially lain down on the top of the flat surface and equilibrated in a solvated environment. Then, one self-assembled dendron **3** micelle[10] was placed in close proximity to the POPC bilayer, the overlapping solvent beads were deleted, and the system was set free to move. These calculations were performed by means of DPD method applying the velocity-Verlet integration algorithm with an integration time step $\Delta t = 0.02\tau$ for a total $8x10^6$ simulation steps. A common way to retrieve the DPD time scale τ is matching the experimental and simulated diffusion constant for water.[15] This yielded a τ of approximately 0.06 ns in our simulations for a total simulation time of approximately 10 μs.

The repulsive interaction parameters between beads a_{ij} were derived from atomistic calculations employing a extensively-validated approach developed by our group,[16-20] assuming the interaction parameter for solvent-solvent interaction $a_{W\text{-}W}$ equal to 25, in harmony with a total bead number density of $\rho = 3/r_c^3$.[8] According to this procedure and as illustrated in detail in our previous DPD simulations of dendron **3**, we employed $a_{PC\text{-}PC}$=25 , $a_{PC\text{-}P}$=27, $a_{PC\text{-}L}$=32, $a_{PC\text{-}C}$=80, $a_{PC\text{-}W}$=21, $a_{P\text{-}P}$=25, $a_{P\text{-}L}$=34, $a_{P\text{-}C}$ = 82, $a_{P\text{-}W}$=15, $a_{L\text{-}L}$=25, $a_{L\text{-}C}$=40, $a_{L\text{-}W}$=33, $a_{C\text{-}C}$=25, $a_{C\text{-}W}$=82. The repulsive interactions between lipids components are $a_{H\text{-}H}$=25, $a_{T\text{-}T}$=25, $a_{H\text{-}T}$=92 and with the solvent $a_{H\text{-}W}$=21 and $a_{T\text{-}W}$=80. The DPD parameters for POPC/dendrimer are $a_{H\text{-}PC}$=29, $a_{H\text{-}P}$=30.3, $a_{H\text{-}L}$= 28, $a_{H\text{-}C}$ = 94, $a_{T\text{-}PC}$ = 57, $a_{T\text{-}P}$ = 44, $a_{T\text{-}L}$= 42, $a_{T\text{-}C}$=23.

In the MBFH calculations the dimensionless Helfand compressibility parameter for the solvent field was fixed to κ_H= 4.6[21] (for $\rho = 3/r_c^3$) and the hybrid bead–field coupling parameters c_{ji} were derived in terms of DPD parameters relying on the relation proposed by Fraaije et al.[21] $c_{ji} = 0.095\Delta a_{ji} + 4.6 = 0.095(a_{ji}\text{-}a_{ii}) + 4.6$, where *j* is a field model, *i* a bead type, and $a_{ii}=a_0$=25.

All simulations were carried out using the software package *Materials Studio* (v. 5.0, Accelrys, San Diego, CA) and *Culgi* (v.9.0, Culgi B.V., Leiden, The Netherlands).

Calculation of zeta potential. We calculated the surface electrostatic potential Ψs of the charged dendron micelles according to the formula:[19, 22]

$$\frac{e\sigma_m}{\kappa\varepsilon_r\varepsilon_0 k_B T} = \Psi_s + \frac{\Psi_s}{\kappa r} - \frac{\tau_1^2 \kappa r}{\tau_2 - \tau_1 \kappa r}$$

where κ is the Debye parameter, σ_m is the micelle surface charge per unit area, ε_0 is the permittivity of vacuum, ε_r corresponds to the relative permittivity, k_BT is the product of the Boltzmann constant and absolute temperature, e is the elementary charge, and:

$$\tau_1 = 2sinh\frac{\Psi_s}{2} - \Psi_s$$

$$\tau_2 = 4tanh\frac{\Psi_s}{4} - \Psi_s$$

Accordingly, the electrostatic potential at the diffuse layer (DL) boundary ζ, known as the zeta potential, was obtained from the Debye-Hückel approximation as:

$$\zeta = \Psi_s \left(\frac{r}{r+\kappa^{-1}}\right) e^{-1}$$

where $(r + \kappa^{-1})$ is the distance of DL boundary from the center of mass of the micelle. The Debye parameter κ in the equation of the electrostatic potential Ψs is obtained from the inverse of Debye length given by:

$$\kappa^{-1} = \sqrt{\frac{\varepsilon_0 \varepsilon_r k_B T}{2N_A e^2 I}}$$

where N_A is Avogadro's number and I is the ionic strength of the solution.

SUPPLEMENTARY FIGURES

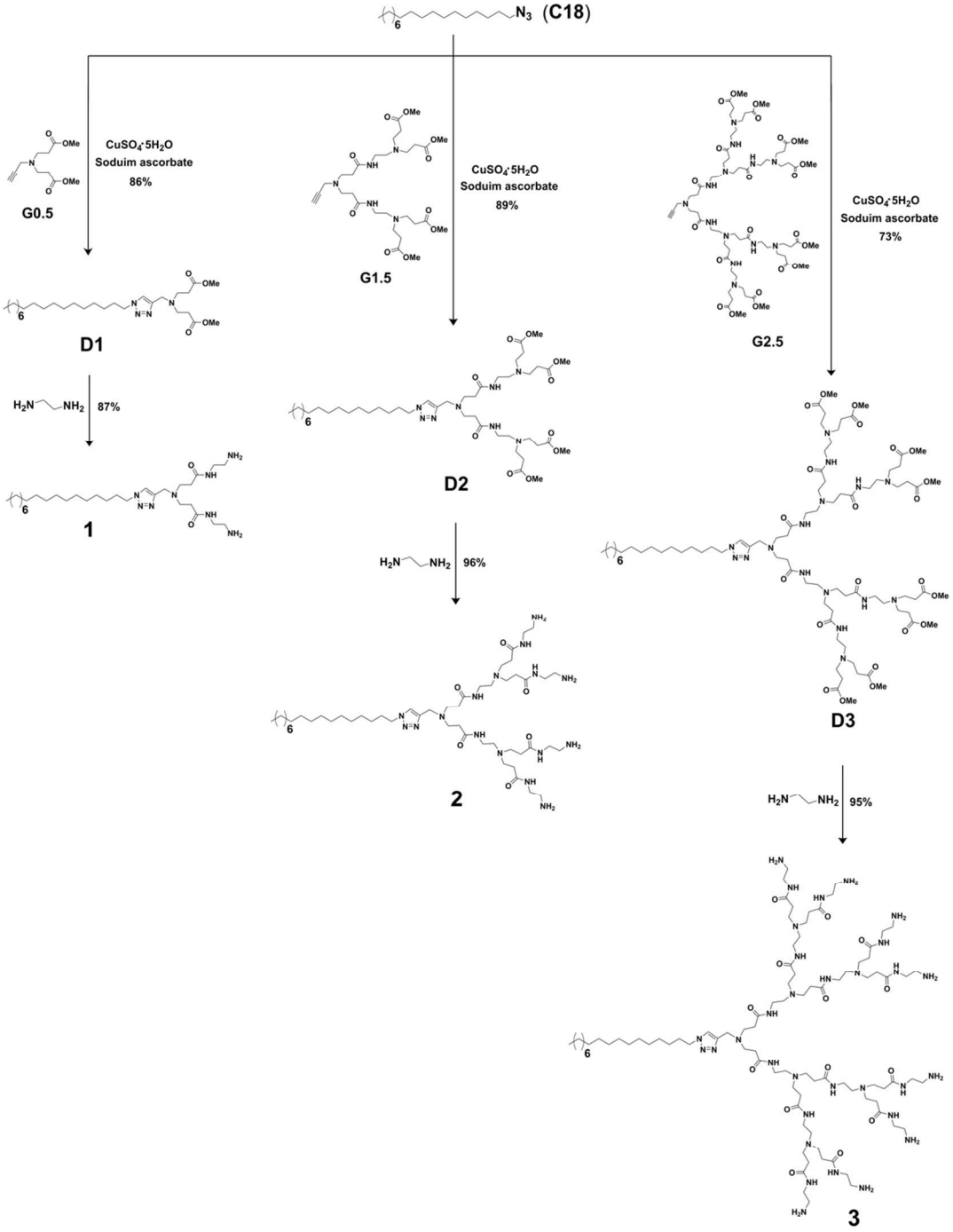

Scheme S1. Synthesis of amphiphilic dendrimers **1** – **3**.

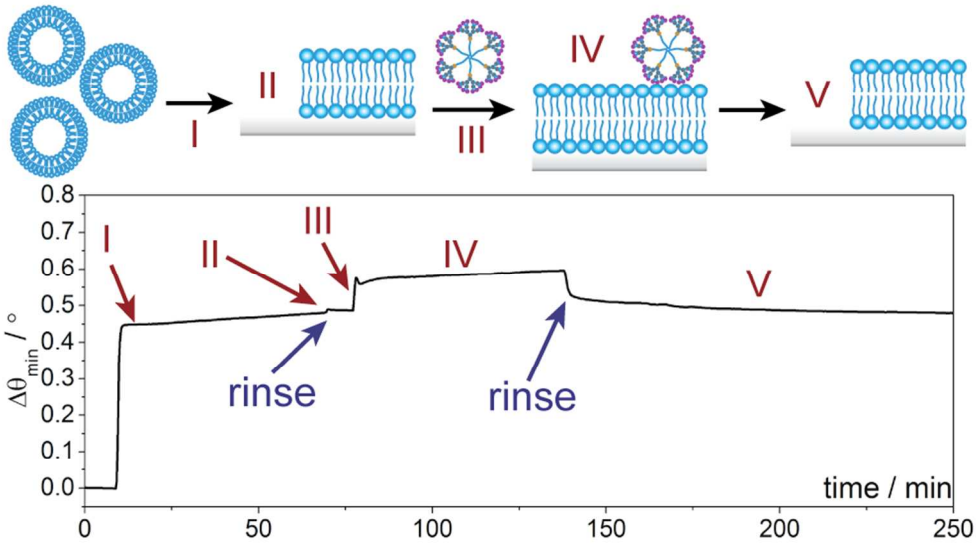

Figure S1. SPR study on fusion of POPC bilayer and transient adsorption of dendrimer **3** micelles with extended rinsing step.

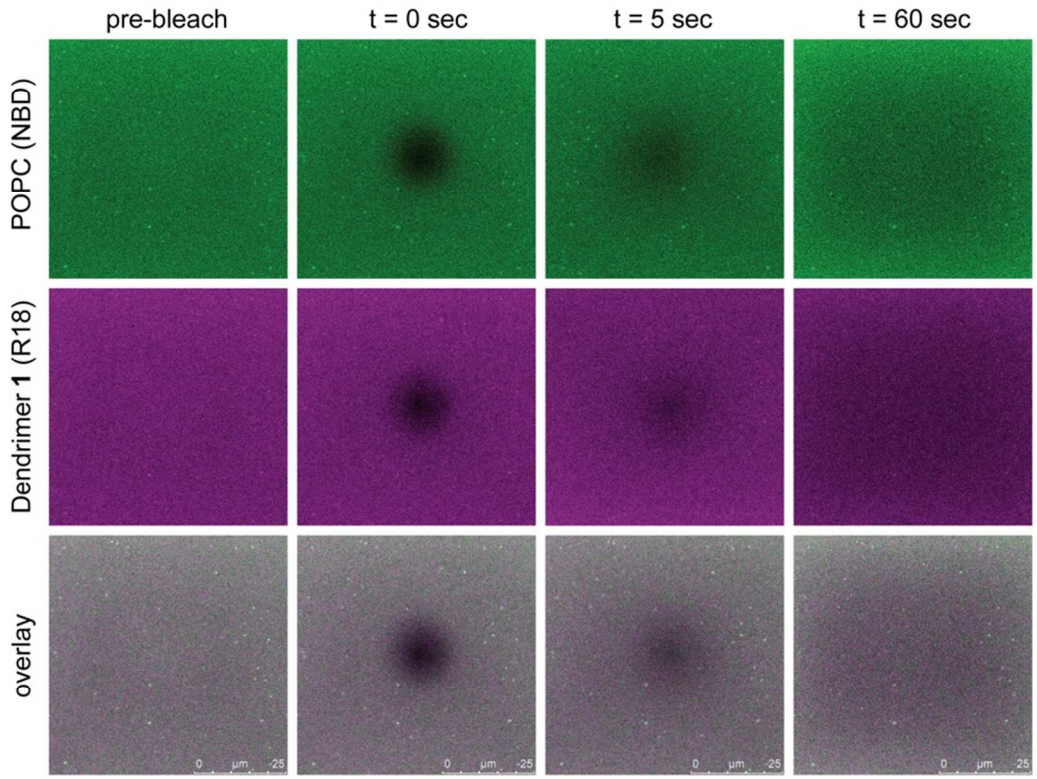

Figure S2. Simultaneous bleaching and recovery of labeled dendrimer micelles and POPC fused within the same membrane. Both areas recover fluorescence within similar amounts of time, indicating integration of both constructs and similar mobilities of each component. Scale bars apply to all images, and represent 25 μm.

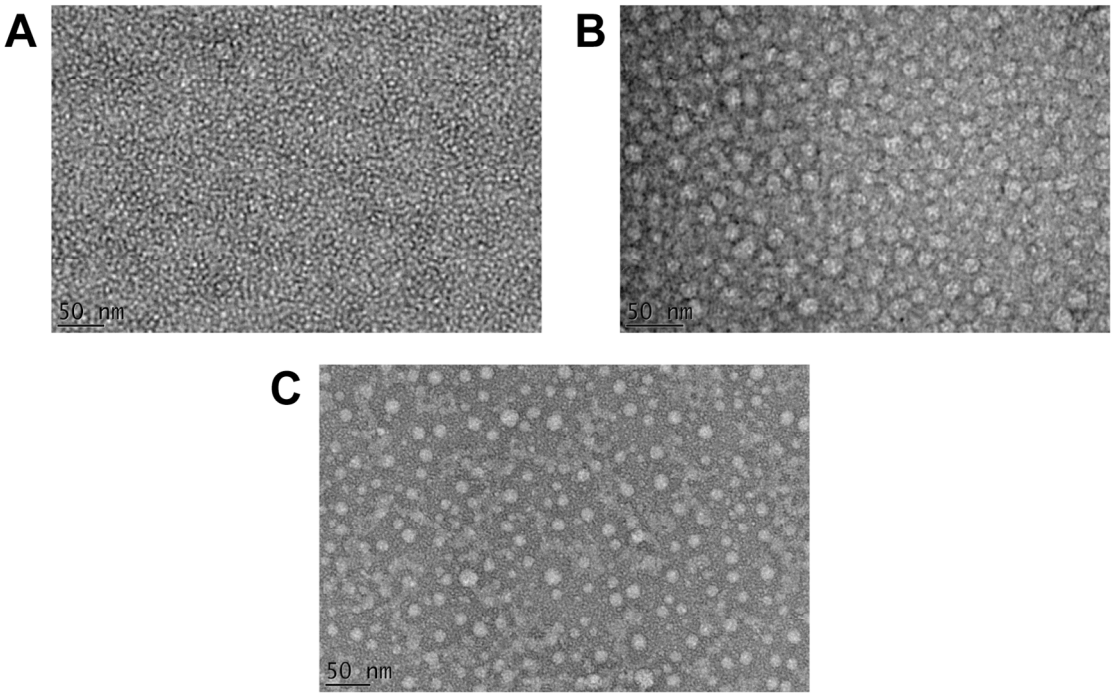

Figure S3. TEM micrographs of dendrimers **1-3** alone assembled into nanomicelles. (A) Dendrimer **1**. (B) Dendrimer **2**. (C) Dendrimer **3**.

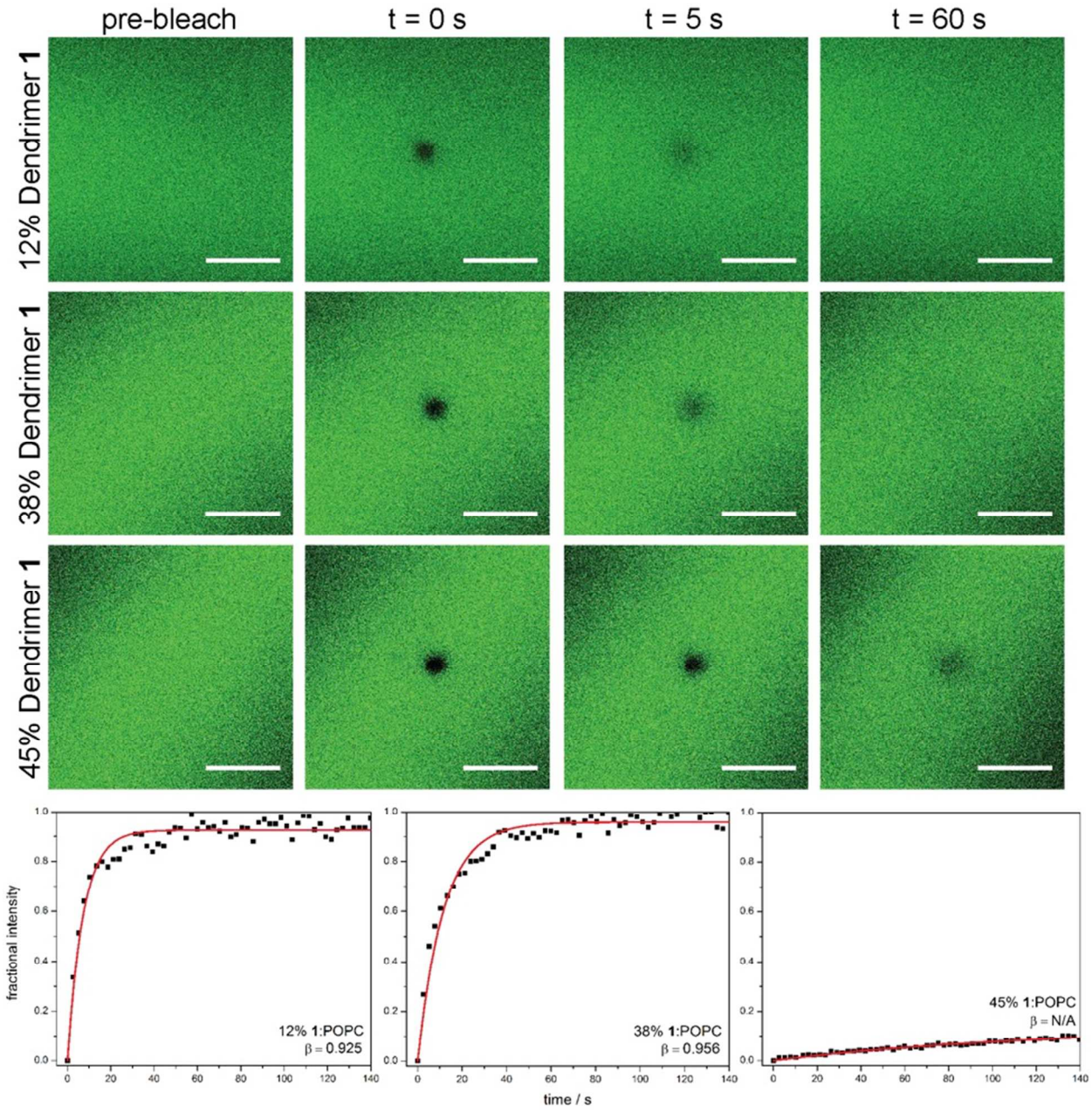

Figure S4. Bleaching and recovery of varying concentrations of dendrimer **1** within POPC membranes. (Top) Fluorescence micrographs, scale bars represent 30 μm. (Bottom) Representative FRAP recovery curves.

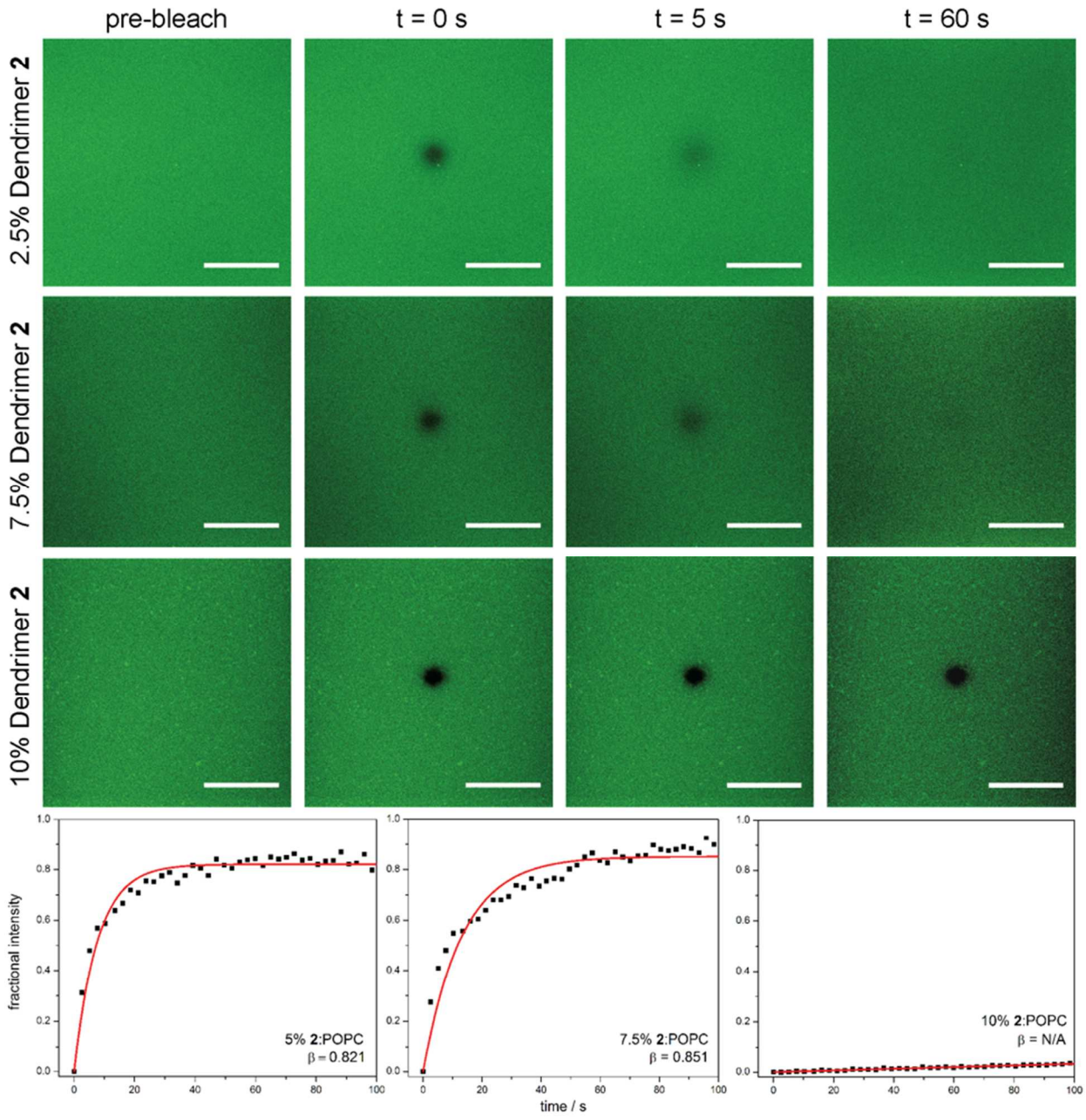

Figure S5. Bleaching and recovery of varying concentrations of dendrimer **2** within POPC membranes. (Top) Fluorescence micrographs, scale bars represent 30 μm. (Bottom) Representative FRAP recovery curves.

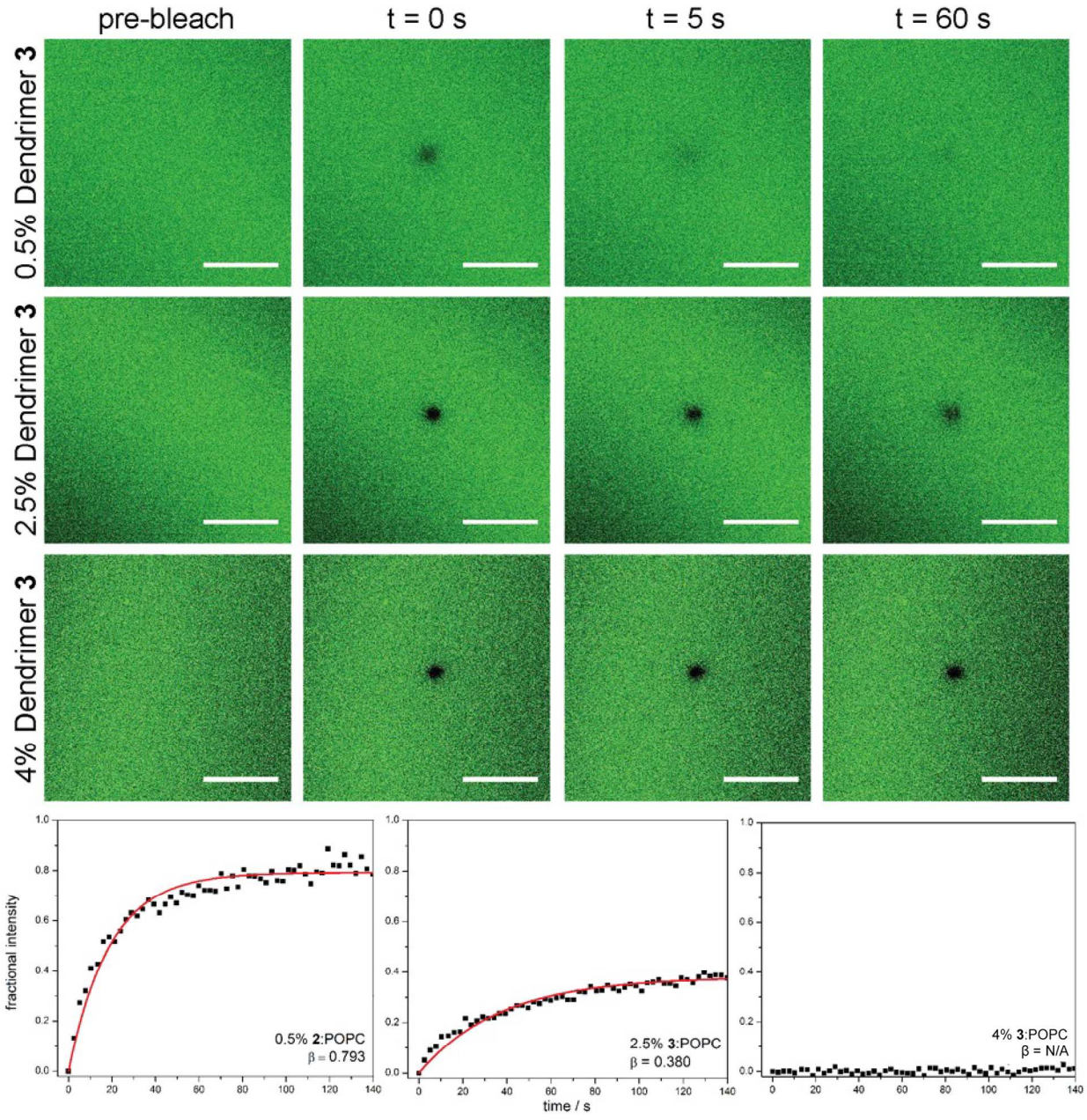

Figure S6. Bleaching and recovery of varying concentrations of dendrimer **3** within POPC membranes. (Top) Fluorescence micrographs, scale bars represent 30 μm. (Bottom) Representative FRAP recovery curves.

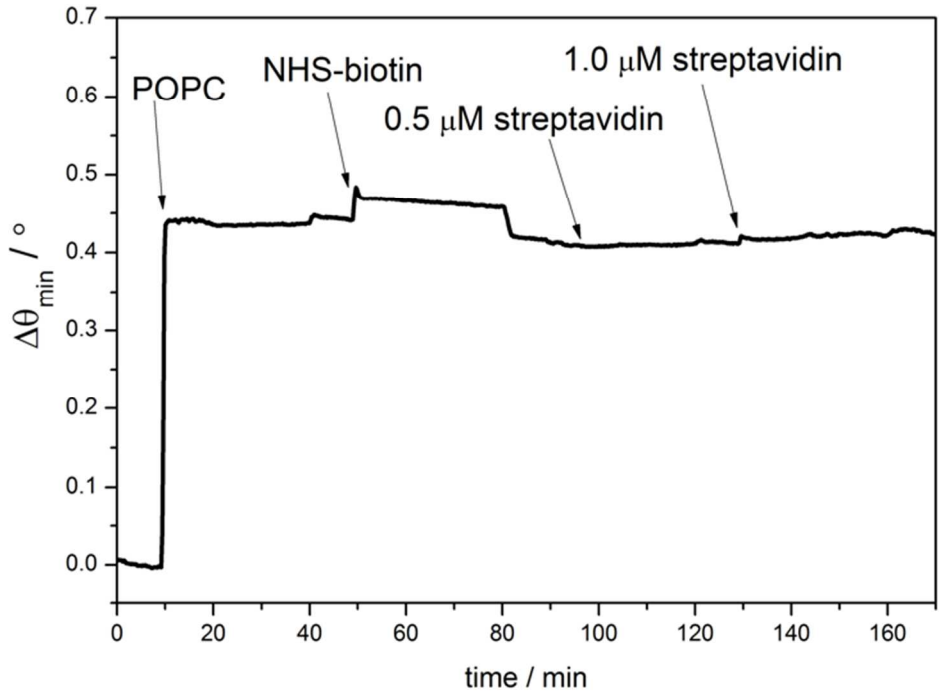

Figure S7. SPR sensorgram depicting attempted derivitization of 100% POPC bilayer with biotin, and streptavidin recognition. There is no increase in resonance angle upon introduction of NHS-biotin or streptavidin, indicating neither interacts with the POPC membrane.

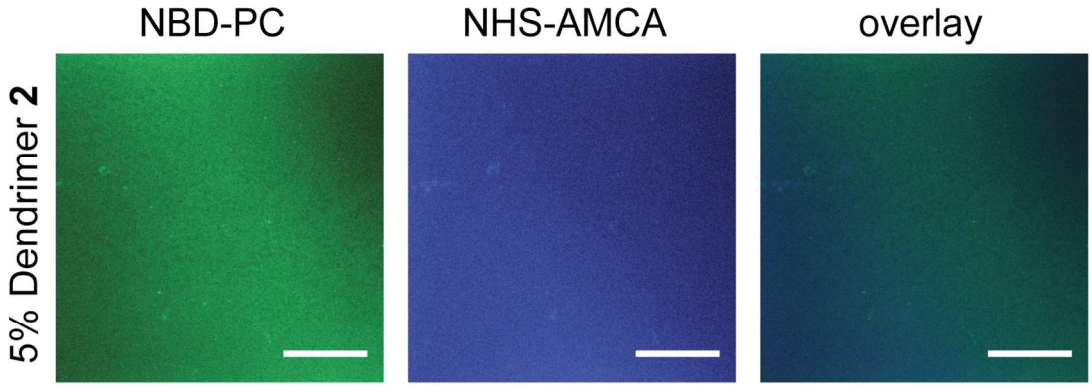

Figure S8. *In situ* derivatization of a 5% **2**/POPC hybrid bilayer with NHS-AMCA. Both the NBD (green, labeled PC) and AMCA (blue, labeled dendrimer) images were acquired over the same region for a **2**/POPC supported lipid bilayer on glass after NHS-AMCA was applied to the membrane for 15 min and thoroughly rinsed with 1×PBS. Scale bars represent 30 μm.

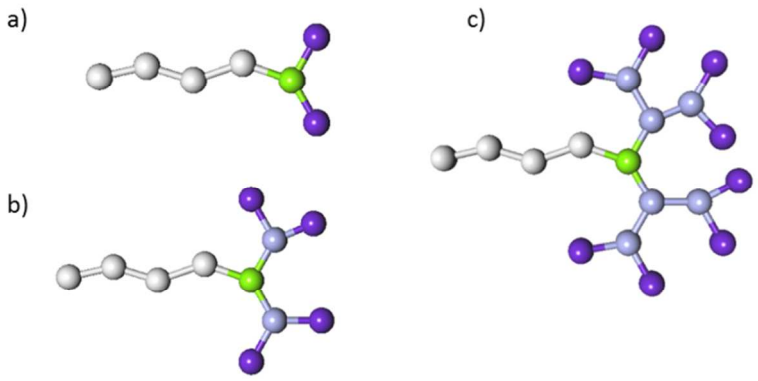

Figure S9. Schematic representation of the coarse-grained DPD models of dendrons **1** (a), **2** (b), and **3** (c). The different bead types are colored as follows: PC, violet blue; P, steel blue; L, chartreuse; C, light gray.

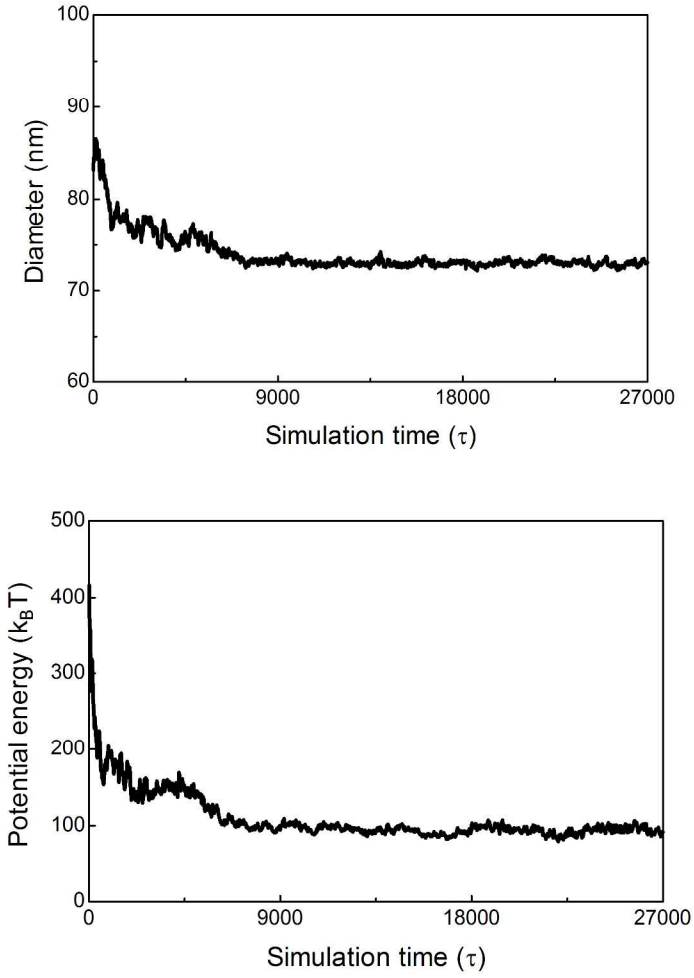

Figure S10. Diameter (top) and potential energy (bottom) as a function of simulation time (τ) for **3**/POPC system equilibration.

SUPPLEMENTARY TABLES

Table S1. Physical properties of hybrid dendrimer/POPC vesicles.

vesicle composition (n/n)[a]	hydrodyn. dia. (nm, ± SEM)	Đ (PDI)	ζ-potential (mV)	mobility ($cm^2/V•s$)
100% POPC	121 ± 6	0.279	0.50	2.80×10^{-6}
5% Dendrimer **1**	108 ± 6	0.285	21.7	1.13×10^{-4}
5% Dendrimer **2**	90 ± 9	0.294	20.9	1.25×10^{-4}
5% Dendrimer **3**	70 ± 4	0.299	24.1	1.09×10^{-4}

[a]Dendrimer percentages (n/n) are relative to POPC content, and total mass concentration for each composition is 1 mg/mL in 1×PBS.

Table S2. Simulated average diameters, surface electrostatic potential (Ψs), and zeta potential (ζ) for the three dendrimer/POPC vesicles.

System	average diameter (nm)	Ψs (mV)	ζ-potential (mV)
1/POPC[a]	105	80.5	22.0
2/POPC[a]	92	79.9	21.6
3/POPC[a]	73	86.5	25.8

[a]The percentage of each dendron in each hybrid vesicle is 5% (n/n), as in real experiments (see Table S1).

SUPPLEMENTARY REFERENCES

(1) Yu, T. Z.; Liu, X. X.; Bolcato-Bellemin, A. L.; Wang, Y.; Liu, C.; Erbacher, P.; Qu, F. Q.; Rocchi, P.; Behr, J. P.; Peng, L. An Amphiphilic Dendrimer for Effective Delivery of Small Interfering RNA and Gene Silencing in Vitro and in Vivo. *Angew. Chem., Int. Ed.* **2012**, *51*, 8478-8484.

(2) Goddard-Borger, E. D.; Stick, R. V. An Efficient, Inexpensive, and Shelf-Stable Diazotransfer Reagent: Imidazole-1-Sulfonyl Azide Hydrochloride. *Org. Lett.* **2007**, *9*, 3797-3800.

(3) Axelrod, D.; Koppel, D. E.; Schlessinger, J.; Elson, E.; Webb, W. W. Mobility Measurement by Analysis of Fluorescence Photobleaching Recovery Kinetics. *Biophys. J.* **1976**, *16*, 1055-1069.

(4) Soumpasis, D. M. Theoretical-Analysis of Fluorescence Photobleaching Recovery Experiments. *Biophys. J.* **1983**, *41*, 95-97.

(5) Hinman, S. S.; Ruiz, C. J.; Drakakaki, G.; Wilkop, T. E.; Cheng, Q. On-Demand Formation of Supported Lipid Membrane Arrays by Trehalose-Assisted Vesicle Delivery for SPR Imaging. *ACS Appl. Mater. Interfaces* **2015**, *7*, 17122-17130.

(6) Murtola, T.; Bunker, A.; Vattulainen, I.; Deserno, M.; Karttunen, M. Multiscale Modeling of Emergent Materials: Biological and Soft Matter. *Phys. Chem. Chem. Phys.* **2009**, *11*, 1869-1892.

(7) Shillcock, J. C. Spontaneous Vesicle Self-Assembly: A Mesoscopic View of Membrane Dynamics. *Langmuir* **2012**, *28*, 541-547.

(8) Groot, R. D.; Warren, P. B. Dissipative Particle Dynamics: Bridging the Gap between Atomistic and Mesoscopic Simulation. *J. Chem. Phys.* **1997**, *107*, 4423-4435.

(9) Sevink, G. J. A.; Fraaije, J. G. E. M. Efficient Solvent-Free Dissipative Particle Dynamics for Lipid Bilayers. *Soft Matter* **2014**, *10*, 5129-5146.

(10) Chen, C.; Posocco, P.; Liu, X.; Cheng, Q.; Laurini, E.; Zhou, J. H.; Liu, C.; Wang, Y.; Tang, J.; Dal Col, V.; Yu, T. Z.; Giorgio, S.; Fermeglia, M.; Qu, F. Q.; Liang, Z.; Rossi, J. J.; Liu, M.; Rocchi, P.; Pricl, S.; Peng, L. Mastering Dendrimer Self-Assembly for Efficient siRNA Delivery: From Conceptual Design to in Vivo Efficient Gene Silencing. *Small* **2016**, *12*, 3667-3676.

(11) Ding, H. M.; Ma, Y. Q. Interactions between Janus Particles and Membranes. *Nanoscale* **2012**, *4*, 1116-1122.

(12) Fraaije, J. G. E. M. Dynamic Density-Functional Theory for Microphase Separation Kinetics of Block-Copolymer Melts. *J. Chem. Phys.* **1993**, *99*, 9202-9212.

(13) Toth, R.; Voorn, D. J.; Handgraaf, J. W.; Fraaije, J. G. E. M.; Fermeglia, M.; Pricl, S.; Posocco, P. Multiscale Computer Simulation Studies of Water-Based Montmorillonite/Poly(Ethylene Oxide) Nanocomposites. *Macromolecules* **2009**, *42*, 8260-8270.

(14) Lindblom, G.; Oradd, G. Lipid Lateral Diffusion and Membrane Heterogeneity. *Biochim. Biophys. Acta* **2009**, *1788*, 234-244.

(15) Groot, R. D.; Rabone, K. L. Mesoscopic Simulation of Cell Membrane Damage, Morphology Change and Rupture by Nonionic Surfactants. *Biophys. J.* **2001**, *81*, 725-736.

(16) Wei, T.; Chen, C.; Liu, J.; Liu, C.; Posocco, P.; Liu, X.; Cheng, Q.; Huo, S.; Liang, Z.; Fermeglia, M.; Pricl, S.; Liang, X. J.; Rocchi, P.; Peng, L. Anticancer Drug Nanomicelles Formed by Self-Assembling Amphiphilic Dendrimer to Combat Cancer Drug Resistance. *Proc. Natl. Acad. Sci. U. S. A.* **2015**, *112*, 2978-2983.

(17) Liu, X. X.; Zhou, J. H.; Yu, T. Z.; Chen, C.; Cheng, Q.; Sengupta, K.; Huang, Y. Y.; Li, H. T.; Liu, C.; Wang, Y.; Posocco, P.; Wang, M. H.; Cui, Q.; Giorgio, S.; Fermeglia, M.; Qu, F. Q.; Pricl, S.; Shi, Y. H.; Liang, Z. C.; Rocchi, P.; Rossi, J. J.; Peng, L. Adaptive Amphiphilic Dendrimer-Based Nanoassemblies as Robust and Versatile siRNA Delivery Systems. *Angew. Chem., Int. Ed.* **2014**, *53*, 11822-11827.
(18) Bromfield, S. M.; Posocco, P.; Chan, C. W.; Calderon, M.; Guimond, S. E.; Turnbull, J. E.; Pricl, S.; Smith, D. K. Nanoscale Self-Assembled Multivalent (SAMul) Heparin Binders in Highly Competitive, Biologically Relevant, Aqueous Media. *Chem. Sci.* **2014**, *5*, 1484-1492.
(19) Barnard, A.; Posocco, P.; Fermeglia, M.; Tschiche, A.; Calderon, M.; Pricl, S.; Smith, D. K. Double-Degradable Responsive Self-Assembled Multivalent Arrays - Temporary Nanoscale Recognition between Dendrons and DNA. *Org. Biomol. Chem.* **2014**, *12*, 446-455.
(20) Jones, S. P.; Gabrielson, N. P.; Wong, C. H.; Chow, H. F.; Pack, D. W.; Posocco, P.; Fermeglia, M.; Pricl, S.; Smith, D. K. Hydrophobically Modified Dendrons: Developing Structure-Activity Relationships for DNA Binding and Gene Transfection. *Mol. Pharmaceutics* **2011**, *8*, 416-429.
(21) Sevink, G. J. A.; Charlaganov, M.; Fraaije, J. G. E. M. Coarse-Grained Hybrid Simulation of Liposomes. *Soft Matter* **2013**, *9*, 2816-2831.
(22) Sader, J. E. Accurate Analytic Formulae for the Far Field Effective Potential and Surface Charge Density of a Uniformly Charged Sphere. *J. Colloid Interface Sci.* **1997**, *188*, 508-510.